

Effect of rough morphology on the flow and heat transfer in nanochannel

Shuting Yao^{1,2}, Jiansheng Wang^{1*}

1 Key Laboratory of Efficient Utilization of Low and Medium Grade Energy, MOE, School of Mechanical Engineering, Tianjin University, Tianjin, 300350, P. R. China

2 College of Petrochemical Technology, Lanzhou University of Technology, Lanzhou, 730050, P. R. China

ABSTRACT

The flow characteristics and heat transfer in rough nanochannel are probed with molecular dynamics. The variations of flow resistance and heat transfer characteristics with rough morphology are investigated. The results show that the smaller nanostructure shear free ratio is beneficial to the heat transfer performance and the drag reduction. In rough channel, the deeper the rough nanostructure grooves, the better the heat transfer, and the greater the flow resistance. The combination of rough morphology and surface wettability will bring a significant impact on the heat transfer performance and drag reduction. In contrast, the rough channel with the weak wall-fluid interaction strength, which characterizes the more hydrophobic surface, has smaller flow resistance and better heat transfer performance.

Keywords: rough morphology; heat transfer; flow characteristics; molecular dynamics

NONMENCLATURE

Symbols

μ	Shear viscosity of fluid, Pa·s
u_x	Fluid velocity, m/s
L_s	Slip length, Å
f	Resistance coefficient
u_m	Mean fluid velocity, m/s
$T_m(x)$	Fluid local mean temperature, K
c	Specific heat capacity, J/kg·K
ρ	Fluid density, kg/m ³

$h(x)$	Heat transfer coefficient, W/(m ² ·K)
λ	Fluid thermal conductivity, W/(m·K)
D_h	Hydraulic diameter, m
T_w	Wall temperature, K
L_k	Temperature jump length, Å
<i>Greek symbols</i>	
ε	Energy parameter, J
σ	Length scale, Å
<i>Subscript</i>	
x, y, z	Coordinate direction
s	Slip
w	Solid wall

1. INTRODUCTION

The applications of micro manufacturing and processing technology have promoted the wide investigations of fluid flow and heat transfer in micro/nano channels or devices [1]. Compared with the conventional channels used in the macroscale systems, when the system dimension is reduced to the nanoscale, channels or devices have a very low hydraulic diameter, which will cause a rather high fluid flow resistance. Besides, the wall-fluid interaction strength becomes more prominent, which will affect the fluid flow and heat transfer in channel dramatically. Thus, it is necessary to observe the interfacial phenomenon from the atomic level. Owing to provide detailed information about flow behavior and thermal transport properties, molecular dynamics simulation gradually becomes a powerful tool to study the flow and heat transfer at the nanoscale.

Although the studies on the nanoscale flow characteristics and heat transfer with molecular dynamics method are sufficiently, they are mainly

focusing on interfacial phenomena and factors influencing on the flow and interface heat transfer [2-5]. In terms of nanoscale convective heat transfer, Markvoort et al. [6] investigated the effect of wall-fluid interaction strength on the convective heat transfer in nanochannel. Ge et al. [7] found that the augment of the wall-fluid interaction strength was conducive to heat transfer. Marable et al. [8] discussed the influences of wall-fluid interaction, channel height, flow velocity and wall temperature on the convective heat transfer. Chakraborty et al. [9] studied the effects of surface roughness and surface coating on the heat transfer performance. Gu et al. [10] studied the effect of axial heat conduction on the heat transfer. Besides, Motlagh et al. [11-12] probed the effects of wall material and nanoparticles on the heat transfer.

However, there are few studies on the flow resistance in nanochannel. One of the most significant factors in nanoscale flow and heat transfer is how to reduce the flow resistance during the heat transfer. That is, we need to consider the heat transfer and flow resistance jointly. The hydrophobic wall has been extensively applied in flow drag reduction due to its larger velocity slip [13-14]. Yet, studies [15-16] have also shown that the drag reduction of hydrophobic wall at the microscale is closely related to the wall roughness. Therefore, the impacts of rough morphology and surface hydrophobic property on the flow resistance and heat transfer characteristics in nanochannel are investigated in present work. The influences of different rough morphologies on flow characteristics and heat transfer in channel with hydrophobic surface are probed.

2. BASIC EQUATIONS AND NUMERICAL PROCESS

2.1 Governing equations

The velocity along the x-direction can be defined as Eq. (1):

$$\mu \frac{\partial^2 u_x}{\partial z^2} = \frac{\partial p}{\partial x} \quad (1)$$

Where μ is shear viscosity. u_x is fluid velocity along the x-direction, $\frac{\partial p}{\partial x}$ is pressure gradient in x direction.

Generally, the slip at the boundary is described by slip length L_s , which is given by:

$$L_s = \frac{u_s}{\left. \frac{\partial u_x}{\partial z} \right|_{z=w}} \quad (2)$$

Where u_s and $\left. \frac{\partial u_x}{\partial z} \right|_{z=w}$ are the slip velocity and fluid velocity gradient at the wall.

The resistance coefficient f and the surface friction coefficient c_f can be calculated as following:

$$f = \frac{\Delta p}{L_x} \frac{D_h}{\frac{1}{2} \rho u_m^2} \quad (3)$$

$$c_f = \frac{\mu \left. \frac{\partial u_x}{\partial z} \right|_{z=w}}{\frac{1}{2} \rho u_m^2} \quad (4)$$

Where $\frac{\Delta p}{L_x}$ is the pressure gradient along the channel. D_h is hydraulic diameter, ρ is fluid density, u_m is fluid mean velocity.

For better comparison, taking the resistance coefficient and the surface friction coefficient corresponding to the smooth channel with the strong wall-fluid interaction as a reference, denoted as f_0 and c_{f0} , the relative resistance coefficient f^* and the relative surface friction coefficient c_f^* are defined as Eq.(5) and Eq.(6).

$$f^* = \frac{f}{f_0} \quad (5)$$

$$c_f^* = \frac{c_f}{c_{f0}} \quad (6)$$

For convective heat transfer, the local mean fluid temperature $T_m(x)$ over the cross-section at different x position is defined as Eq. (7), and the local heat transfer coefficient $h(x)$ can be obtained as Eq. (8). The local Nusselt number Nu_x can be calculated from Eq. (10) by combining Eq. (8) and Eq. (9).

$$T_m(x) = \frac{\int_0^H c \rho u_x(x, z) T(x, z) dz}{\int_0^H c \rho u_x(x, z) dz} \quad (7)$$

$$h(x) = \frac{\lambda}{(T_m(x) - T_w)} \left. \frac{\partial T}{\partial z} \right|_{z=w} \quad (8)$$

$$Nu_x = \frac{h(x)D_h}{\lambda} \quad (9)$$

$$Nu_x = \frac{D_h}{(T_m(x) - T_w)} \left. \frac{\partial T}{\partial z} \right|_{z=w} \quad (10)$$

Where c is specific heat capacity, $T(x, z)$ is fluid temperature along the x -direction. λ is thermal conductivity, T_w is wall temperature. $\left. \frac{\partial T}{\partial z} \right|_{z=w}$ is fluid temperature gradient at the wall-fluid interface.

The temperature jump length L_k can also be defined as:

$$L_k = \frac{\Delta T}{\left. \frac{\partial T}{\partial z} \right|_{z=w}} \quad (11)$$

Here, ΔT is the temperature jump at the wall-fluid interface.

2.2 Simulation details

As shown in Fig.1, the channel size is $415 \times 60 \times 120 \text{ \AA}^3$ and the channel height is $H=120 \text{ \AA}$. Each solid wall is composed of platinum atoms with a thickness of $D=20 \text{ \AA}$. The argon atoms are used to set as fluid in nanochannel, and the fluid density is 1200 kg/m^3 . The Langevin thermostat is used to keep the solid wall at specified temperature of 200K. The fluid domain is divided into three regions shown in Fig. 1: force region, thermostat region and sample collection region. The force region is applied to the x -directional coordinates of $-15 \text{ \AA} < x < -10 \text{ \AA}$, and a driving force of $F_{\text{ext}}=2.4 \text{ pN}$ is imposed to the fluid atoms located in force region. Temperature resetting is performed only for fluid atoms inside the region of $-10 \text{ \AA} < x < 0 \text{ \AA}$ without disturbing the directional flow [7, 9]. After temperature resetting, an initial temperature of 300K is generated at inlet. Periodic boundary conditions are applied in the x - and y -directions, respectively. The entire system is firstly relaxed in canonical ensemble at 200K. After reaching the steady state with an external driving force, the simulation data is used for sampling, averaging and data collection. All simulation cases are performed with a timestep of 1fs.

The Lennard-Jones (LJ) 12-6 potential model is used to describe the interaction between the atoms. Where i, j correspond to interacting atoms, respectively. ϵ is energy parameter and σ is length scale for LJ potential function. r_c is cutoff radius, $r_c=10 \text{ \AA}$. For the fluid-fluid interaction, $\epsilon_1=1.67 \times 10^{-21} \text{ J}$, $\sigma_1=3.405 \text{ \AA}$. For the wall-wall interaction: $\epsilon_s=8.35 \times 10^{-20} \text{ J}$, $\sigma_s=2.475 \text{ \AA}$. Here, $m_l=6.63 \times 10^{-26} \text{ kg}$, $m_s=3.24 \times 10^{-25} \text{ kg}$. For the wall-fluid

interaction, $\sigma_{sl}=2.87 \text{ \AA}$, the ϵ_{sl} are $1.0\epsilon_l$ and $0.25\epsilon_l$, which characterizes the strong and weak wall-fluid interaction.

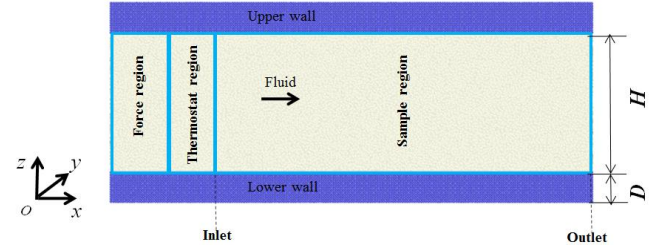


Fig 1 Schematic model of computational domain

Fig.2 shows the rough morphology in nanochannel. Here, w is the groove width, h is the groove depth and s is the groove spacing. The nanostructure shear free ratio is defined as: $\phi_a = \frac{w}{w+s}$. To investigate the effect of nanostructure depth on the flow and heat transfer characteristics, the different nanostructure depths are 4 \AA and 16 \AA , respectively. A series of nanostructure dimensions under different nanostructure shear free ratios are listed in Tab.1.

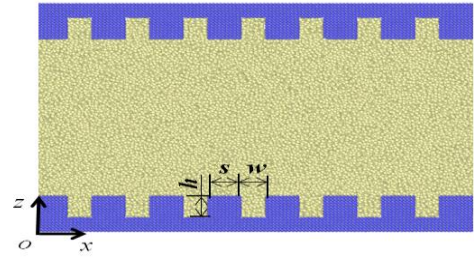


Fig 2 Rough nanostructure morphology

Tab.1 Nanostructure dimension parameters under different shear free ratios

ϕ_a	w	s	h	h
0.1875	6 \AA	26 \AA		
0.25	8 \AA	24 \AA		
0.375	12 \AA	20 \AA	4 \AA	16 \AA
0.5	16 \AA	16 \AA		
0.75	24 \AA	8 \AA		

3. RESULTS AND DISCUSSION

3.1 Development of velocity and temperature

As shown in Fig.3, the fluid flow is in fully developed condition, and the fluid velocity at the different x positions is almost constant. It's found that the mean velocity in smooth channel with the weak wall-fluid interaction is greater than that in smooth channel with the strong wall-fluid interaction by comparing Fig.3 (a) and Fig.3 (b). The weak wall-fluid interaction strength means that wall surface is more difficult to wet, which is closer to the properties of

hydrophobic surface. The fluid atoms move more freely near the wall. As a result, the mean velocity corresponding to the weak wall-fluid interaction is greater.

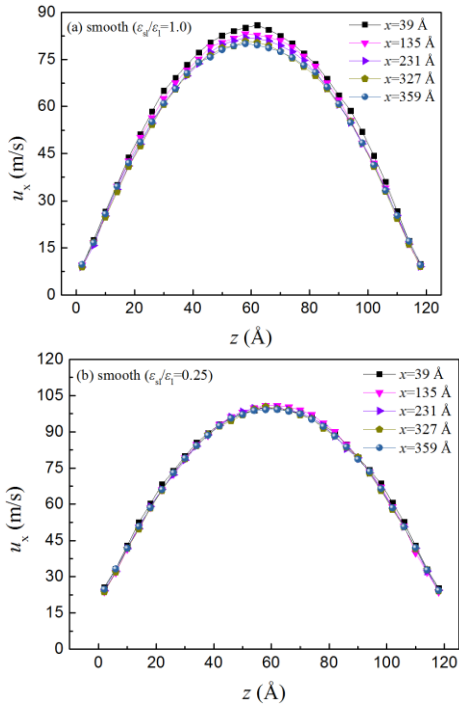


Fig 3 Velocity profiles along the flow direction

Fig.4 shows the fluid temperature distribution along the smooth channel. Obviously, when the fluid flows along the channel, the flow is in the thermally developing firstly and finally reaches the thermal-fully developed condition. Correspondingly, the fluid temperature along the x direction firstly decreases, and then the temperature profiles are almost overlapping and invariable. Moreover, the fluid temperature in smooth channel with the strong wall-fluid interaction strength at the thermal-fully developed state is lower, which indicates that the strong wall-fluid interaction strength is beneficial to heat transfer in the channel and makes the heat transfer more sufficient.

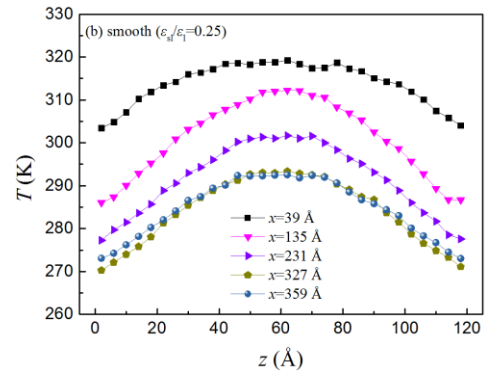
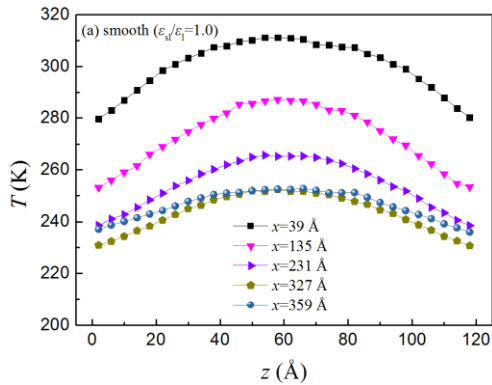


Fig 4 Temperature profiles along the flow direction

3.2 Effect of rough morphology on heat transfer and flow resistance

When the flow and thermal are fully developed, the variations of thermal parameters in the channel corresponding to weak wall-fluid interaction strength are shown in Fig.5. The rough nanostructure decreases temperature jump at the wall-fluid interface. As a result, the Nusselt number in rough channel is greater than that in smooth channel, and the Nusselt number in rough channel decreases with the increase of nanostructure shear free ratio. In addition, as the rough nanostructure depth increases, the temperature jump decreases while the Nusselt number increases gradually. It indicates that the deeper nanostructure grooves enhance the heat transfer between solid wall and fluid.

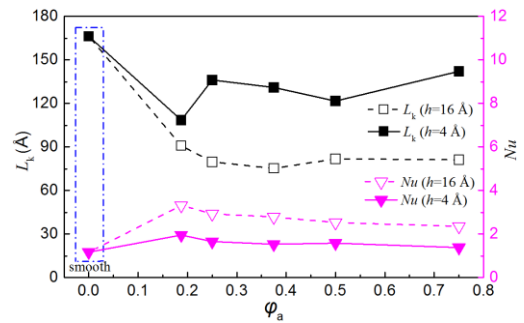


Fig 5 Variation trends of thermal parameters

Fig.6 shows the variations of flow characteristics parameters in the channel when the flow and thermal are fully developed. Under the condition of the weak wall-fluid interaction, the relative resistance coefficient and relative surface friction coefficient in rough channel are higher due to the existence of the rough morphology. Moreover, the relative resistance coefficient and relative surface friction coefficient increase gradually as the nanostructure shear free ratio increases. According to Fig.6 (a) and Fig.6 (b), under the same nanostructure shear free ratio, the augment of rough nanostructure depth increases the flow resistance due to the decrease of velocity slip. Thus,

Tab.2 Variation rates of the Nusselt number and resistance coefficient

Nanostructure depth	Parameters	φ_a					
		0(smooth)	0.1875	0.25	0.375	0.5	0.75
$h=4\text{\AA}$	Nu	41.3%↓	1.8%↓	16.8%↓	22.9%↓	20.4%↓	30.7%↓
	f^*	43.7%↓	27.1%↓	21.8%↓	15.9%↓	12.4%↓	7.8%↓
$h=16\text{\AA}$	Nu	41.3%↓	66.4%↑	47.2%↑	39.9%↑	27.3%↑	18.5%↑
	f^*	43.7%↓	2.1%↑	8.9%↑	23.5%↑	36.2%↑	49.2%↑

the smaller nanostructure shear free ratio and the smaller nanostructure depth are beneficial to the reduction of the flow resistance in rough channel.

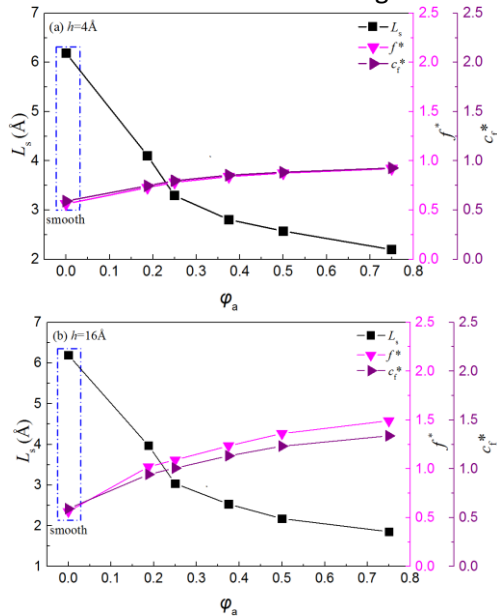


Fig 6 Variation trends of flow characteristics parameters

Tab.2 shows the influence of rough morphology on the Nusselt number and resistance coefficient in channel with weak wall-fluid interaction. Compared with the parameters in smooth channel with strong wall-fluid interaction, both the Nusselt number and the relative resistance coefficient in smooth channel with weak wall-fluid interaction decrease as shown in Tab.2, and the relative resistance in rough channel corresponding to nanostructure depth of 4\AA also decreases, which indicates they have better drag reduction characteristics. Yet, under the weak wall-fluid interaction, the decrease rate of Nusselt number in rough channel with nanostructure depth of 4\AA is much lower than the decrease rate of Nusselt number in smooth channel. Although the Nusselt number of rough channel with nanostructure depth of 16\AA increases greatly, but the corresponding relative resistance coefficient is also mostly increased. Therefore, the increase of nanostructure depth will weaken the drag reduction characteristics. The rough channel

corresponding to nanostructure depth of 4\AA has better heat transfer and drag reduction characteristics.

4. CONCLUSIONS

In present work, a three-dimensional model of convective heat transfer in nanochannel is established to investigate the influences of rough morphology on the heat transfer and flow resistance characteristics. The conclusions are drawn as following:

(1)The rough channel with weak wall-fluid interaction possesses better drag reduction characteristics and heat transfer performance.

(2)The rough morphology plays a significant role in affecting the flow resistance and heat transfer at the wall-fluid interface. The smaller nanostructure shear free ratio is conducive to obtain the better heat transfer and drag reduction jointly.

(3)The larger rough nanostructure depth is conducive to the heat transfer, but not beneficial to the drag reduction due to the constraints on fluid atoms derived from the nanostructure grooves.

ACKNOWLEDGEMENT

The authors gratefully acknowledge the financial support by the Key Natural Science Foundation of Tianjin (No.17JCZDJC31200).

REFERENCE

- [1] O. Mahian, L. Kolsi, M. Amani, P. Estellé, et al., Recent advances in modeling and simulation of nanofluid flows—Part II: Applications. Physics Reports, 791(2019) 1-59.
- [2] F. C. Wang, Y. P. Zhao, Slip boundary conditions based on molecular kinetic theory: The critical shear stress and the energy dissipation at the liquid-solid interface, Soft Matter. 7(18) (2011) 8628-8634.
- [3] H. Hu, Y. Sun, Effect of nanopatterns on Kapitza resistance at a water-gold interface during boiling: A molecular dynamics study. Journal of Applied Physics, 112(5) (2012)053508.
- [4] M. Barisik, A. Beskok, Temperature dependence of thermal resistance at the water/silicon interface.

International Journal of Thermal Sciences, 77(2014)47-54.

[5] H. Rahmatipour, A. Azimian, O. Atlaschian, Study of fluid flow behavior in smooth and rough nanochannels through oscillatory wall by molecular dynamics simulation. *Physica A: Statistical Mechanics and its Applications*, 465(2017)159-174.

[6] A.J. Markvoort, P. Hilbers, S. Nedeja, Molecular dynamics study of the influence of wall-gas interactions on heat flow in nanochannels, *Phys. Rev. E*, 71 (6) (2005)066702.

[7] S. Ge, Y. Gu, M. Chen, A molecular dynamics simulation on the convective heat transfer in nanochannels, *Mol. Phys.* 113 (7) (2015)703–710.

[8] D. C. Marable, S. Shin, A. YousefzadiNobakht, Investigation into the microscopic mechanisms influencing convective heat transfer of water flow in grapheme nanochannels. *International Journal of Heat and Mass Transfer*, 109(2017)28-39.

[9] P. Chakraborty, T. F. Ma, L. Cao, Y. Wang, Significantly enhanced convective heat transfer through surface modification in nanochannels. *International Journal of Heat and Mass Transfer*, 136(2019)702-708.

[10] Y.W. Gu, S. Ge, M. Chen, A molecular dynamics simulation of nanoscale convective heat transfer with the effect of axial heat conduction, *Mol. Phys.* 114 (12) (2016)1922–1930.

[11] M. B. Motlagh, M. Kalteh, Investigating the wall effect on convective heat transfer in a nanochannel by molecular dynamics simulation. *International Journal of Thermal Sciences*, 156(2020)106472.

[12] M. B. Motlagh, M. Kalteh, Molecular dynamics simulation of nanofluid convective heat transfer in a nanochannel: Effect of nanoparticles shape, aggregation and wall roughness. *Journal of Molecular Liquids*, 318(2020)114028.

[13] B. Wang, J. D. Wang, Z. L. Dou, et al. Investigation of Retention of Gases in Transverse Hydrophobic Microgrooved Surfaces for Drag Reduction. *Ocean Engineering*, 79(2014)58-66.

[14] B. R. K. Gruncell, N. D. Sandham, G. Mchale, Simulations of Laminar Flow Past a Super hydrophobic Sphere with Drag Reduction and Separation Delay. *Physics of Fluids*, 25(4) (2013)043601.

[15] E. Aljallis , M. A. Sarshar, R. Datla, et al. Experimental Study of Skin Friction Drag Reduction on Superhydrophobic Flat Plates in High Reynolds Number Boundary Layer Flow. *Physics of Fluids*, 25(2) (2013)025103-025114.

[16] H. Park, H. Park, J. Kim, A Numerical Study of the Effects of Super hydrophobic Surface on Skin-Friction Drag in Turbulent Channel Flow. *Physics of Fluids*, 25(11) (2013)110815.

Enerarxiv-preprint